Compatibility in Blends of Two Random Copolymers Having a Common Monomer Segment

Tomoo Shiomi,† Frank E. Karasz,* and William J. MacKnight

Department of Polymer Science and Engineering, University of Massachusetts, Amherst, Massachusetts 01003. *Received March 6, 1986*

ABSTRACT: Miscibility in blends of random copolymers $(A_xB_{1-x})_{r_1}$ and $(C_yB_{1-y})_{r_2}$ can conveniently be displayed as domains in a Cartesian coordinate system in which the abscissa and ordinate represent the compositions of the respective copolymers. For the case in which the two copolymers have a common monomer unit (e.g., B) the isothermal boundary between domains of miscibility and immiscibility in a mean field treatment is determined by three segmental interaction parameters, χ_{AB}, χ_{AC}, and χ_{BC}, and the degrees of polymerization r_1 and r_2 of the copolymers. We have termed such representations "miscibility maps". The shape and size of the miscibility domain are determined by the relationships between these parameters, and the present study considers the various theoretical possibilities with interpretations based on intersegmental repulsion and/or attraction. In addition, two experimental miscibility maps for blends of poly(vinyl chloride-*co*-vinyl acetate) with chlorinated poly(vinyl chloride) (regarded here as a random copolymer of vinyl chloride and 1,2-dichloroethylene units) and poly(vinyl chloride-*co*-vinyl acetate) with poly(ethylene-*co*-vinyl acetate) were constructed by using as a criterion of miscibility the glass transition temperatures determined by scanning calorimetry. The boundary defining the region of miscibility for the blend of poly(vinyl chloride-*co*-vinyl acetate) with chlorinated poly(vinyl chloride) was elliptical and that for the poly(vinyl chloride-*co*-vinyl acetate)/poly(ethylene-*co*-vinyl acetate) blend was defined by a pair of hyperbolas. Segmental interaction parameters between the different monomer units were estimated from these data and good correlation was obtained between theoretical evaluations and experiment. In addition the experimental miscibility map obtained by Hall et al. for blends of poly(styrene-*co*-maleic anhydride) with poly(styrene-*co*-acrylonitrile) was compared to the theoretical calculations.

Introduction

The study of polymer blends has been extensively developed in recent years.[1-3] Although compatibility is unusual in blend systems of high molecular weight polymers because of the very small combinatorial entropy, a number of compatible polymer pairs have been found.[1-3] According to recent theories of polymer miscibility,[4-7] the Gibbs free energy of mixing contains three contributions: the combinatorial entropy of mixing, the exchange interaction, and a free volume term. When the contribution of the exothermic exchange interaction term is larger than the free volume term, which contributes positively to the Gibbs free energy, two polymers may be miscible. As the temperature is increased, the contribution of the free volume term to the free energy increases and phase separation may occur at an elevated temperature, the lower critical solution temperature (LCST). Therefore, a specific interaction between two polymers favors miscibility.

Recently it has been demonstrated[8-18] that systems consisting of a homopolymer and a copolymer may be miscible for a certain range of copolymer composition even though the combinations of their corresponding homopolymers are immiscible. For example, poly(2,6-dimethyl-1,4-phenylene oxide) (PPO) is not miscible with either poly(*o*-fluorostyrene) or poly(*p*-fluorostyrene) but is miscible with poly(*o*-fluorostyrene-*co*-*p*-fluorostyrene) within a certain copolymer composition range.[14] These systems have no exothermic interaction between the different monomer units. Such a "miscibility window" is due to a repulsion between the two different monomer units comprising the copolymer,[18,19] and in a mean field approach the overall Flory–Huggins interaction parameter between the two polymers can be simply expressed in terms of the respective segmental χ_{ij}'s. ten Brinke et al.[20] extended this formulation to mixtures of two different copolymers and also discussed the temperature dependence of miscibility.

In the general case of blends of two copolymers the miscibility region at a particular temperature can be displayed as domains in a Cartesian coordinate system in which the axes represent the copolymer compositions; e.g., for mixtures of $(A_xB_{1-x})_{r_1}$ and $(C_yD_{1-y})_{r_2}$ the copolymer compositions are represented on the ordinate and abscissa with $0 \leq x, y \leq 1$. We have termed these representations "miscibility maps". The size and shape of the miscibility domains are governed in the general case by the relationships between the six segmental interaction parameters χ_{ij} representing all possible binary interactions and the degrees of polymerization r_1 and r_2. In the special case D ≡ B in which the two copolymers possess a common monomer, the number of independent χ_{ij} is reduced to three.

This paper consists of two sections; section I discusses the theoretical miscibility maps for the special case of blends of two random copolymers having a common monomer, e.g., $(A_xB_{1-x})_{r_1}$ and $(C_yB_{1-y})_{r_2}$. As indicated above, the boundaries of the miscibility domains are a function of the signs and relative magnitudes of the three segmental interaction parameters and of r_1 and r_2; representative combinations of χ_{ij} are presented and the resulting miscibility maps are discussed in terms of the repulsive or attractive forces between the respective monomer units. In section II experimental miscibility maps are shown for two blend systems of copolymers having a common monomer and are used to estimate the segmental χ_{ij} parameters for these blends. In the last part of section II experimental data from the literature[17] are again compared to the theoretical calculations.

I. Theoretical Section

In the first-order Flory–Huggins formulation for polymer mixing,[21] the free energy of mixing ΔG at a temperature T for a blend of $r_1$mers and $r_2$mers can be written

$$\Delta G/RT = (\phi_1/r_1) \ln \phi_1 + (\phi_2/r_2) \ln \phi_2 + \chi_{blend}\phi_1\phi_2 \quad (1)$$

where R is the gas constant, ϕ_1 and ϕ_2 are the volume fractions of $r_1$mer and $r_2$mer in the blend, and χ_{blend} is the net segmental interaction parameter between the two

† Permanent address: Department of Materials Science and Technology, Technological University of Nagaoka, Nagaoka, Niigata 949-54, Japan.

0024-9297/86/2219-2274$01.50/0

polymers. For blends of two random copolymers, according to ten Brinke, Karasz, and MacKnight,[20] χ_{blend} can be written as a general quadratic equation whose variables are the compositions, x and y, of the two copolymers expressed in volume fractions. For blends of the copolymers $(A_xB_{1-x})_{r_1}$ and $(C_yB_{1-y})_{r_2}$ χ_{blend} is given by

$$\chi_{blend} = \chi_{AB}x^2 + (\chi_{AC} - \chi_{BC} - \chi_{AB})xy + \chi_{BC}y^2 \quad (2)$$

where χ_{AB}, χ_{BC}, and χ_{AC} are the segmental χ parameters between the different monomer units as indicated by their subscripts. The function $f(x,y)$ will be defined by

$$f(x,y) \equiv \chi_{blend} - \chi_{crit} \quad (3)$$

where the conformational entropy term χ_{crit} is given by

$$\chi_{crit} = \tfrac{1}{2}(r_1^{-1/2} + r_2^{-1/2})^2 \quad (4)$$

It may be noted that the segmental χ_{ij} appropiate to these expression are implicitly functions of the specific mers chosen to represent the basic repeat unit of the respective polymers. In the convention followed here, $r_{1,2}$ represents the degrees of polymerization as normally defined for the polymers and the χ_{ij} will therefore be applicable for ij interactions of any combination of mers in which this convention is followed.

The miscibility or immiscibility of the blend is determined by the sign of $f(x,y)$; the region of miscibility is defined by $f(x,y) < 0$ and (for the cases considered here) always includes the origin 0,0, and the region of immiscibility is defined by $f(x,y) > 0$. Thus the solution of eq 3 represents the miscibility boundary in the $0 \leq x, y \leq 1$ domain. The miscibility–immiscibility boundary also represents the consolute point for the blend of the two copolymers whose compositions x, y lie on the boundary, while the composition of the blend itself, i.e., the volume ratios of the two copolymers constituting the mixture, are given by the usual Flory–Huggins solution of this problem. It is well-known theoretically and experimentally that for mixtures of two polymers of comparable molecular weights the critical blend composition contains approximately equal volumes of the components.

As is obvious from eq 2 and 3, $f(x,y) = 0$ may describe a point, a straight line, or two intersecting straight lines for the case $\chi_{crit} = 0$, corresponding to a blend of infinite molecular weight copolymers. For $\chi_{crit} > 0$ (i.e., blends of finite molecular weight copolymers) the miscibility boundaries will be described by an ellipse or a circle that includes the origin or by a pair of hyperbolas symmetrically located with respect to the asymptotes passing through the origin.

Results and Discussion

Calculated Miscibility Maps. As indicated above there are a substantial number of possible miscibility maps corresponding to the conditions expressed by eq 2 and 3. Each condition can be written in three identical forms with respect to χ_{AB}, χ_{BC}, and χ_{AC}, and there is an obvious symmetry with respect to the first two of these; for convenience the expression with respect to the magnitude of χ_{AB} alone is discussed in the text, while the equivalent expressions are listed in Appendix I.

The miscibility maps described below are isothermal sections through a three-dimensional volume whose surface represents the miscibility/immiscibility boundary in terms of copolymer composition and temperature. In all the diagrams presented the shaded areas represent miscibility for finite molecular weight systems while the smaller region, defined by solid lines, represents miscibility in the infinite molecular weight limit. Although the major purpose of these diagrams is schematic, they were each calculated with appropriate numerical values, which are listed in Appendix II.

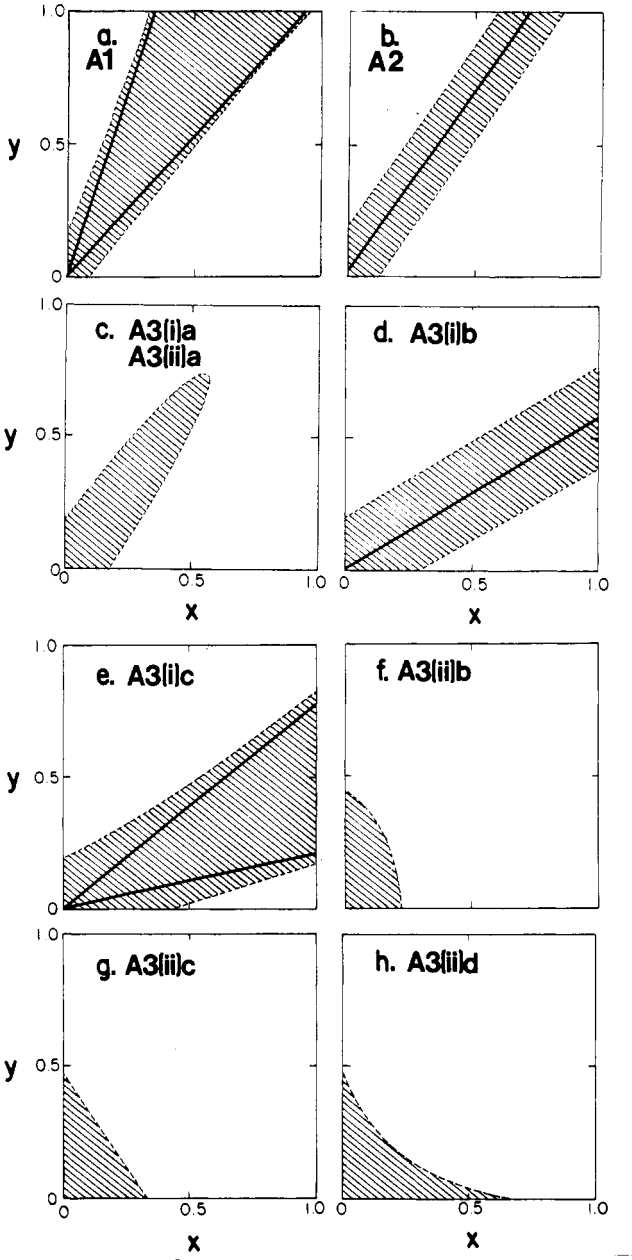

Figure 1. Theoretical miscibility maps for the case of $\chi_{ij} > 0$ for all ij. The x and y axes represent the compositions of the copolymers $(A_xB_{1-x})_{r_1}$ and $(C_yB_{1-y})_{r_2}$, respectively. The solid lines contain the regimes of miscibility for infinite molecular weight polymers and the shaded area corresponds to miscibility for blends of the finite molecular weight polymers. Boundaries were calculated with eq 2 and 3, and the χ_{ij} values given in Appendix II and fulfilling the conditions described in the text and in Appendix I; $\chi_{crit} = 0.002$ throughout. The conditions described in the text to which the figures correspond are indicated.

The possible miscibility maps are grouped overall according to the signs of the individual χ_{ij}.

A. All $\chi_{ij} > 0$. In this case there are eight different miscibility maps; all are shown in Figure 1.

1. $\chi_{AB} > (\chi_{BC}^{1/2} + \chi_{AC}^{1/2})^2$. Figure 1a shows a miscibility region exists even for blends of polymers of infinite molecular weights; in this case this region is defined by two straight lines. For blends of finite molecular weight copolymers, the miscibility region is enlarged by the two symmetrically disposed hyperbolas. Thus, although there are repulsive interactions between every pair of monomer units in the copolymer, repulsion between the monomer

units A and B in effect predominates and provides a miscibility region, as argued recently for the copolymer/homopolymer case.[18-20] Indeed, for the particular χ_{ij} chosen to yield Figure 1a the miscibility range is widest at $y = 1$, corresponding to the blend of the copolymer $(A_xB_{1-x})_{r_1}$ with the homopolymer C_{r_2}. As the content of the monomer B in the copolymer $(C_yB_{1-y})_{r_2}$ is increased, this range narrows resulting from the fact that the net intermolecular attraction decreases as the increasing repulsive intramolecular interaction between C and B partially offsets the A–B intramolecular interaction in the respective copolymers.

2. $\chi_{AB} = (\chi_{BC}^{1/2} + \chi_{AC}^{1/2})^2$. As the magnitude of χ_{AB} decreases, the miscibility region narrows. Finally, in the case of the equality shown above, miscibility is reduced to a straight line passing through the origin for the infinite molecular weight limit. For blends of copolymers with finite molecular weights, the miscibility region lies between the two straight lines of equal slope, as indicated in Figure 1b.

3. As χ_{AB} is decreased further, the following two situations exist with respect to the magnitudes of the other χ_{ij}:

(i) $\chi_{BC} > \chi_{AC}$.

a. $(\chi_{BC}^{1/2} - \chi_{AC}^{1/2})^2 < \chi_{AB} < (\chi_{BC}^{1/2} + \chi_{AC}^{1/2})^2$

Figure 1c shows that in this case, for blends of finite molecular weight copolymers, the miscibility region is contained by an ellipse whose major axis has a positive slope and is unity when $\chi_{AB} = \chi_{BC}$. There is no miscibility for infinite molecular weight blends. Such an elliptical miscibility region again may be said to result from repulsive interactions, even though the repulsion is weaker than that in case A2. Characteristically the elliptical miscibility domain is enlarged with a decrease of molecular weights. The miscibility maps for condition A3(i)a are in contrast to another situation, in which χ_{AC} is relatively large, described below.

b. $\chi_{AB} = (\chi_{BC}^{1/2} - \chi_{AB}^{1/2})^2$

Figure 1d, corresponding to the condition A3(i)b, again indicates that a single line represents the miscibility in the infinite molecular weight limit, broadened as indicated for the finite molecular weight system. If the inequality in A3(i)c holds

c. $\chi_{AB} < (\chi_{BC}^{1/2} - \chi_{AC}^{1/2})^2$

the miscibility map is of the type shown in Figure 1e. We note that conditions A3(i)b and A3(i)c are equivalent to $\chi_{BC} \geq (\chi_{AB}^{1/2} + \chi_{AC}^{1/2})^2$, which emphasizes the necessity for a sufficiently large χ_{BC}.

(ii) $\chi_{BC} < \chi_{AC}$.

a. $\chi_{AC} - \chi_{BC} < \chi_{AB} < (\chi_{BC}^{1/2} + \chi_{AC}^{1/2})^2$

The result is identical with that depicted in Figure 1c.

b. $(\chi_{AC}^{1/2} - \chi_{BC}^{1/2})^2 < \chi_{AB} < \chi_{AC} - \chi_{BC}$

For this case the miscibility region is contained by an ellipse with a negative slope of its major axis as shown in Figure 1f. As is obvious from condition A3(ii)b, in this case χ_{AC} is larger than the sum of χ_{AB} and χ_{BC}.

c. $\chi_{AB} = (\chi_{AC}^{1/2} - \chi_{BC}^{1/2})^2$

For this case the boundary between the miscibility and immiscibility regions is again represented by a straight line for finite molecular weight systems; miscibility is limited to the origin for the infinite molecular weight case; see Figure 1g.

d. $\chi_{AB} < (\chi_{AC}^{1/2} - \chi_{BC}^{1/2})^2$

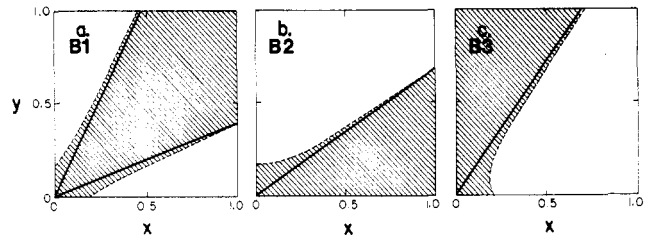

Figure 2. Theoretical miscibility maps for two $\chi_{ij} > 0$. See the caption for Figure 1 for explanation.

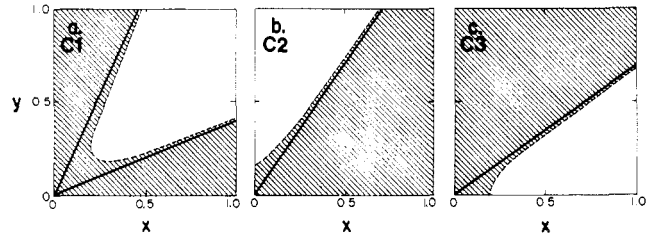

Figure 3. Theoretical miscibility maps for one $\chi_{ij} > 0$. See the caption for Figure 1 for explanation.

This condition results in the domain depicted in Figure 1h, in which the asymptote to the hyperbola forming the boundary of the domain passes through the origin with negative slope, which emphasizes that condition A3(ii)d is equivalent also to $\chi_{AC} > (\chi_{AB}^{1/2} + \chi_{BC}^{1/2})^2$. Here intermolecular repulsion predominantes over intramolecular repulsion.

B. Two $\chi_{ij} > 0$. In this case, there are fewer possibilities than for case A.

1. $\chi_{AC} < 0$; χ_{AB}, $\chi_{BC} > 0$. In this case (Figure 2a) the miscibility domain includes the point x, $y = 1$ corresponding to the miscibility of the homopolymers of A and C.

2. $\chi_{AB} < 0$; $\chi_{A,C}$ $\chi_{BC} > 0$. 3. $\chi_{BC} < 0$; χ_{AC}, $\chi_{AB} > 0$. In Figure 2, parts b and c, (conditions B2 and B3, respectively) the miscibility domains are contained by the axes $y = 0$, $x = 0$, respectively, as a consequence of the respective negative χ_{ij}.

C. One $\chi_{ij} > 0$. In this case, three miscibility maps can be found as shown in Figure 3.

1. $\chi_{AC} > 0$; χ_{AB}, $\chi_{BC} < 0$. In this case (Figure 3a) the *immiscibility* domain includes x, $y = 1$ corresponding to the immiscibility of the homopolymers A and C, while the miscibility domain includes the axes $x = 0$ and $y = 0$ because the homopolymer B is miscible with both copolymers $(A_xB_{1-x})_{r_1}$ and $(C_yB_{1-y})_{r_2}$.

2. $\chi_{BC} > 0$; χ_{AC}, $\chi_{AB} < 0$. 3. $\chi_{AB} > 0$; χ_{AC}, $\chi_{BC} < 0$. In Figure 3, parts b and c, (for conditions C2 and C3) the miscibility domain again includes the point x, $y = 1$ as required by the condition $\chi_{AC} < 0$.

D. All $\chi_{ij} < 0$. Even though all χ_{ij} are negative, a domain of immiscibility will be found if $|\chi_{AB}|$ is large enough to fulfill condition D1 (as shown in Figure 4a).

1. $\chi_{AB} \leq -(|\chi_{BC}|^{1/2} + |\chi_{AC}|^{1/2})^2$. In the infinite molecular weight case, the two rectilinear boundaries containing the immiscibility region merge for the equality D1 and immiscibility is then limited to a single line passing through the origin. Immiscibility results from the attractive effect of the two different monomer units of the copolymers, which prevails over the attractive interaction of A and C, in contrast to the repulsive effect described above. An analogous situation (a "window of immiscibility") is discussed for the homopolymer/copolymer blend case in ref 20.

2. When the absolute values of χ_{AB} or χ_{BC} are not sufficiently large with respect to that of χ_{AC}, for example

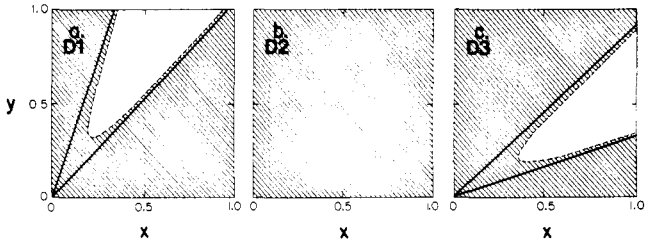

Figure 4. Theoretical miscibility maps for $\chi_{ij} < 0$ for all ij. See the caption for Figure 1 for explanation.

Table I
Vinyl Acetate Contents and Molecular Weights of Polymers Used

sample	VAc content, wt %	VAc content, mol %	$\bar{M}_w \times 10^5$	$\bar{M}_n \times 10^5$
PVC-1			2.1	1.3
PVC-2			0.46	0.23
PVC-3			1.2	0.72
poly(VC-*co*-VAc-1)	2.5	1.8	1.6	0.94
poly(VC-*co*-VAc-2)	10	7.5	0.91	0.43
poly(VC-*co*-VAc-3)	13	9.8	0.26	0.13
poly(VC-*co*-VAc-4)	19[a]	14.6[a]	0.37	0.23
poly(Et-*co*-VAc-1)	87.1	68.7	2.0	0.67
poly(Et-*co*-VAc-2)	83.2	61.7	1.6	0.55
poly(Et-*co*-VAc-3)	79.5	55.8	1.7	0.60
poly(Et-*co*-VAc-4)	70	43	2.2	0.66
poly(Et-*co*-VAc-5)	50	25	2.4	0.93
poly(Et-*co*-VAc-6)	45	21	2.8	1.1
poly(Et-*co*-VAc-7)	40	18	0.88	0.41

[a] Including maleic acid.

if $\chi_{AB} \geq -(|\chi_{BC}|^{1/2} + |\chi_{AC}|^{1/2})^2$ and $\chi_{BC} > \chi_{AC}$ or $-(|\chi_{BC}|^{1/2} + |\chi_{AC}|^{1/2})^2 < \chi_{AB} < -(|\chi_{BC}|^{1/2}\,|\chi_{AC}|^{1/2})^2$, the two copolymers are miscible over the entire ranges of the copolymer composition, Figure 4b.

3. $\chi_{BC} < -(|\chi_{AB}|^{1/2} + |\chi_{AC}|^{1/2})^2$. If this condition is fulfilled an immiscibility domain is again found (Figure 4c).

II. Experimental Section

In this section the above considerations are applied to three systems of copolymer blends, each containing a common monomer moiety. The data for two of these systems, poly(vinyl acetate-*co*-vinyl chloride)/chlorinated poly(vinyl chloride) and poly(vinyl chloride-*co*-vinyl acetate)/poly(ethylene-*co*-vinyl acetate) were experimentally obtained in the present study; the analysis of the third case, poly(styrene-*co*-maleic anhydride)/poly(styrene-*co*-acrylonitrile) was made on the basis of measurements carried out by Hall et al.[17]

Samples. Details of poly(vinyl chloride) homopolymers (PVC), vinyl chloride–vinyl acetate copolymers (poly(VC-*co*-VAc)) and ethylene–vinyl acetate copolymers (poly(Et-*co*-VAc)) used are listed in Table I. PVC-1 and -2 were supplied by BFGoodrich Co., and PVC-3 and poly(VC-*co*-VAc-1) through poly(VC-*co*-VAc-4) were obtained from Polysciences, Ltd., and Scientific Polymer Products, Inc., respectively. Poly(Et-*co*-VAc-1) through poly(Et-*co*-VAc-3) and poly(Et-*co*-VAc-4) through poly(Et-*co*-VAc-6) (Levapren 700, 500, and 400) were supplied by Kuraray Co., Japan, and by Bayer, Germany, respectively. Poly(Et-*co*-VAc-7) was obtained from Scientific Polymer Products, Inc. The vinyl acetate contents of all the copolymers shown in Table I are nominal, and poly(VC-*co*-VAc-4) also contains 2 wt % maleic acid. The molecular weights of all the samples were determined by GPC in tetrahydrofuran (THF), relative to polystyrene standards. Chlorinated PVC's (CPVC) (Table II) were prepared from PVC-1 and characterized (by BFGoodrich) as described elsewhere.[22] The weight percent chlorine contents of the CPVC samples are shown in Table II. The differing molecular weights and molecular weight distributions of the samples from various origins resulted in relatively minor inconsistencies in the comparisons of miscibilities of different systems ultimately reflected in uncertainties in the analysis.

Table II
Chlorine and CHCl.CHCl Contents of CPVC Samples

sample	chlorine content, wt %	content of CHCl.CHCl unit, mol %
CPVC-1	61.9	22.5
CPVC-2	62.3	24.6
CPVC-3	63.7	31.9
CPVC-4	64.2	34.7
CPVC-5	64.4	35.8
CPVC-6	65.5	42.2
CPVC-7	68.5	61.6

Measurements. All blends were prepared by casting from a common solvent, THF. The two constituent polymers were dissolved in the solvent (2.5% (w/v)) at a blend ratio of 50/50 wt %; all solutions were clear. The solvent was allowed to evaporate at room temperature and the resulting film was dried under vacuum for at least 3 days at 70 °C.

The compatibilities of the respective blends were assessed as a function of annealing temperature (i.e., thermal history) in the normal manner by determining the presence or absence of two glass transition temperatures, using a Perkin-Elmer DSC-4 differential scanning calorimeter. Annealing of the samples was carried out in the DSC. In a typical experiment a sample was heated at 320 °C/min to a selected temperature and annealed for the desired time. After annealing it was cooled at 320 °C/min to an initial temperature of scanning. The thermal analyses were then carried out at a heating rate of 20 °C/min, using sample sizes of 15–20 mg. The compatibilities of certain blends containing poly(Et-*co*-VAc-5) to poly(Et-*co*-VAc-7) (50, 45, and 40 wt % VAc contents) were determined by the disappearance of the T_g of the other constituent polymer present in the blends because the thermograms of these Et–VAc copolymers showed broad peaks in a temperature range of ca. −30 to +60 °C caused by the melting of crystallites. Both the shapes and the temperature ranges of the peaks were similar to those observed for Levapren 450M (45 wt % VAc) by Elmquist and Svanson.[23]

Results

Experimental Miscibility Maps. In this section the three experimental miscibility maps will be compared to the theoretically calculated domains.

1. **Poly(vinyl acetate-*co*-vinyl chloride)/Chlorinated Poly(vinyl chloride).** The CPVC polymers can be regarded as random copolymers containing the two monomer units, CHCl.CHCl (ClVC) and CH_2.CHCl (VC), with the assumption that the presence of other chlorinated VC units can be neglected. This assumption is probably valid for CPVC with a low degree of chlorination.[24]

The 50/50 wt % blends of the copolymers $(VAc)_x(VC)_{1-x}$ and $(ClVC)_y(VC)_{1-y}$ were annealed for 1 h at temperatures above the glass transition of CPVC. Figure 5 shows the miscibility map obtained by observing the T_g's for the samples at various temperatures (see the caption for Figure 5). Miscibility is represented as a function of the mole fractions of the two copolymer compositions. In figure 5, $y = 0$ for CPVC and $x = 0$ for poly(VC-*co*-VAc) correspond to the PVC homopolymer representing the limiting compositions for both systems. In obtaining the experimental data, sample PVC-1 was used for studies of blends with the vinyl acetate copolymers, i.e., along the axis $y = 0$, while samples of PVC-1 and -2 were used in the blends with the chlorinated PVC copolymers ($x = 0$).

The polymer PVC-1 ($\bar{M}_w = 2.1 \times 10^5$) was miscible only with CPVC-1, while PVC-2 ($\bar{M}_w = 4.6 \times 10^4$) because of its lower molecular weight was miscible with CPVC-1 as well as CPVC-2. Also, the blend of poly(VC-*co*-VAc-1) and CPVC-2 was miscible at 120 °C but immiscible at 135, 150, and 180 °C (even though the miscibility of all the other blends was independent of the annealing temperature), which indicates, therefore, that in this system the consolute point is of the LCST type. As shown in Figure 5, the

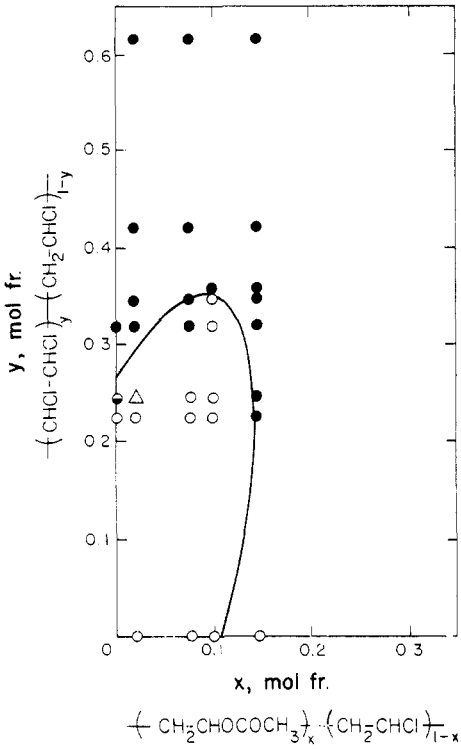

Figure 5. Miscibility regimes for blends of VC/VAc and CPVC copolymers: (○) miscible; (●) immiscible. The point shown by (◒) represents miscibility for the PVC-2/CPVC blend but immiscibility for the PVC-1/CPVC blend. The point labelled (△) represents miscibility at 120 °C but immiscibility at 135, 150, and 180 °C. The annealing temperatures were 120, 135, 150 and 180 °C for the blend containing PVC-1, CPVC-1 and -2, 150 and 180 °C for the blends containing CPVC-3 to -6, and 180 °C for those containing CPVC-7. The best fit solid line was calculated with the χ_{ij} values shown in Table III and $\chi_{crit} = 0.0031$.

Table III
Segmental Interaction Parameters[a]

segment pair	χ_{ij}	segment pair	χ_{ij}
VAc.ClVC	0.17	VC.ClVC	0.042
VAc.VC	0.27	VC.Et	0.15
VAc.Et	1.01		

[a] The values are calculated for an average temperature of 150 °C. Uncertainty is estimated to be ±20%.

miscibility region is best contained by an ellipse qualitatively similar to that depicted in Figure 1c in section I of this paper. Theory predicts this system to be immiscible in the infinite molecular weight limit.

The solid line in Figure 5 is a boundary line calculated with eq 2–4, in which volume fractions of the monomer units were assumed to be equal to the mole fractions. The value of χ_{crit} was estimated to be 0.0031 from the number-average degrees of polymerization using eq. 4. We took $r_1 = 2100$ for all the CPVC polymers; this was assumed to be equal to r_1 for PVC-1 because of the origin of the CPVC polymers. For the VC–VAc copolymers, $r_2 = 310$, averaged for PVC-2, poly(VC-*co*-VAc-3) and poly(VC-*co*-VAc-4). The miscibility boundary is a best fit of the data using the derived χ_{ij} values for $\chi_{VAc\cdot VC}$, $\chi_{ClVC\cdot VC}$ and $\chi_{VAc\cdot ClVC}$ listed in Table III. Since the annealing temperatures were 150–180 °C the calculated curve and the segmental χ_{ij} obtained can be regarded as corresponding to this temperature range.

2. Poly(vinyl chloride-*co*-vinyl acetate)/Poly(ethylene-*co*-vinyl acetate). Figure 6 shows the miscibility map obtained from observation of T_g's for the blends of poly(VC-*co*-VAc) and poly(Et-*co*-VAc). The

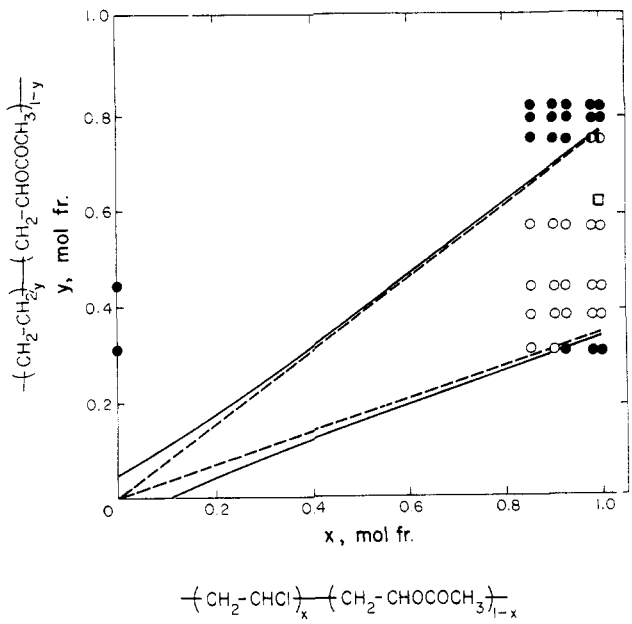

Figure 6. Miscibility regimes for blends of poly(VC-*co*-VAc) and poly(Et-*co*-VAc) copolymers annealed at 100, 130, and 160 °C: (○) miscible; (●) immiscible; (◑) miscible at 100 and 130 °C but immiscible at 160 °C; (□) miscible, obtained by Hammer.[10] The solid and broken lines were calculated with the χ_{ij} values shown in Table III; the former is for the finite molecular weight blends ($\chi_{crit} = 0.0021$) and the latter for the infinite molecular weight blends ($\chi_{crit} = 0$).

homopolymer PVC-3 was used in these blends for $x = 1$. The blends of poly(Et-*co*-VAc-5) with PVC-3 and with poly(VC-*co*-VAc-1) were miscible at 100 and 130 °C but were immiscible at 160 °C, which again demonstrates that these systems display an LCST. The poly(vinyl chloride) homopolymer is miscible with the Et–VAc copolymers with a VAc content of 50–83.2 wt % (25–61.7 mol %) at 100 and 130 °C. In agreement with the results shown in Figure 6, Hammer[10] showed that this system was miscible in a range of VAc content of 60–75 wt %, and Elmquist and Svanson[23] reported that it was immiscible at the VAc content of 45 wt %.

As is obvious from comparison of the observed and theoretical miscibility maps, Figure 6 corresponds to the cases depicted in Figure 1a or 1e. The immiscibility/miscibility boundaries are a function of the three segmental interaction parameters $\chi_{VC\cdot VAc}$, $\chi_{Et\cdot VAc}$ and $\chi_{Et\cdot VC}$, and χ_{crit}. The value of χ_{crit} of 0.0021 for this system was estimated from the number-average degrees of polymerization $r_1 = 780$ averaged for PVC-3 and the four VC–VAc copolymers and $r_2 = 1400$ averaged for all the Et–VAc copolymers. The parameter $\chi_{VC\cdot VAc}$ was already available from the analysis of the poly(VC-*co*-VAc)/CPVC blends. The remaining two χ_{ij} were obtained by a best fit of the PVC/poly(Et-*co*-VAc) data. The χ_{ij} values thus obtained are also listed in Table III. The boundaries calculated with the above χ_{ij} are shown by the broken and solid lines in Figure 6. The broken lines correspond to blends of polymers with infinite molecular weights ($\chi_{crit} = 0$), and the solid lines indicate blends of copolymers of average molecular weights corresponding to those used experimentally.

3. Poly(styrene-*co*-maleic anhydride)/Poly(styrene-*co*-acrylonitrile). Recently Paul and Barlow[19] analyzed the miscibility of blends of random copolymers and applied their analysis to data obtained for the blends of poly(styrene-*co*-maleic anhydride) poly(S-*co*-MA) and poly(styrene-*co*-acrylonitrile) poly(S-*co*-AN) copolymers described by Hall et al.[17] Their analysis was carried out

Table IV

designation in text	condition	Figure
A1	1. $\chi_{AB} > (\chi_{BC}^{1/2} + \chi_{AC}^{1/2})^2$	
	2. $\chi_{BC} < (\chi_{AB}^{1/2} - \chi_{AC}^{1/2})^2$; $\chi_{AB} > \chi_{AC}$	1a
	3. $\chi_{AC} < (\chi_{AB}^{1/2} - \chi_{BC}^{1/2})^2$; $\chi_{AB} > \chi_{BC}$	
A2	1. $\chi_{AB} = (\chi_{BC}^{1/2} + \chi_{AC}^{1/2})^2$	
	2. $\chi_{BC} = (\chi_{AB}^{1/2} - \chi_{AC}^{1/2})^2$; $\chi_{AB} > \chi_{AC}$	1b
	3. $\chi_{AC} = (\chi_{AB}^{1/2} - \chi_{BC}^{1/2})^2$; $\chi_{AB} > \chi_{BC}$	
A3(i)a and A3(ii)a	1. $(\chi_{BC}^{1/2} - \chi_{AC}^{1/2})^2 < \chi_{AB} < (\chi_{BC}^{1/2} + \chi_{AC}^{1/2})^2$; $\chi_{BC} > \chi_{AC}$	
	1′. $\chi_{AC} - \chi_{BC} < \chi_{AB} < (\chi_{BC}^{1/2} + \chi_{AC}^{1/2})^2$; $\chi_{BC} < \chi_{AC}$	
	2. $(\chi_{AB}^{1/2} - \chi_{AC}^{1/2})^2 < \chi_{BC} < (\chi_{AB}^{1/2} + \chi_{AC}^{1/2})^2$; $\chi_{AB} > \chi_{AC}$	1c
	2′. $\chi_{AC} - \chi_{AB} < \chi_{BC} < (\chi_{AB}^{1/2} + \chi_{AC}^{1/2})^2$; $\chi_{AB} < \chi_{AC}$	
	3. $(\chi_{AB}^{1/2} - \chi_{BC}^{1/2})^2 < \chi_{AC} < \chi_{AB} + \chi_{BC}$	
A3(i)b	1. $\chi_{AB} = (\chi_{BC}^{1/2} - \chi_{AC}^{1/2})^2$; $\chi_{BC} > \chi_{AC}$	
	2. $\chi_{BC} = (\chi_{AB}^{1/2} + \chi_{AC}^{1/2})^2$	1d
	3. $\chi_{AC} = (\chi_{AB}^{1/2} - \chi_{BC}^{1/2})^2$; $\chi_{BC} > \chi_{AB}$	
A3(i)c	1. $\chi_{AB} < (\chi_{BC}^{1/2} - \chi_{AC}^{1/2})^2$; $\chi_{BC} > \chi_{AC}$	
	2. $\chi_{BC} > (\chi_{AB}^{1/2} + \chi_{AC}^{1/2})^2$	1e
	3. $\chi_{AC} < (\chi_{AB}^{1/2} - \chi_{BC}^{1/2})^2$; $\chi_{BC} > \chi_{AB}$	
A3(ii)b	1. $(\chi_{AC}^{1/2} - \chi_{BC}^{1/2})^2 < \chi_{AB} < \chi_{AC} - \chi_{BC}$; $\chi_{AC} > \chi_{BC}$	
	2. $(\chi_{AC}^{1/2} - \chi_{AB}^{1/2})^2 < \chi_{BC} < \chi_{AC} - \chi_{AB}$; $\chi_{AC} > \chi_{AB}$	1f
	3. $\chi_{AB} + \chi_{BC} < \chi_{AC} < (\chi_{AB}^{1/2} + \chi_{BC}^{1/2})^2$	
A3(ii)c	1. $\chi_{AB} = (\chi_{AC}^{1/2} - \chi_{BC}^{1/2})^2$; $\chi_{AC} > \chi_{BC}$	
	2. $\chi_{BC} = (\chi_{AC}^{1/2} - \chi_{AB}^{1/2})^2$; $\chi_{AC} > \chi_{AB}$	1g
	3. $\chi_{AC} = (\chi_{AB}^{1/2} + \chi_{BC}^{1/2})^2$	
A3(ii)d	1. $\chi_{AB} < (\chi_{AC}^{1/2} - \chi_{BC}^{1/2})^2$; $\chi_{AC} > \chi_{BC}$	
	2. $\chi_{BC} < (\chi_{AC}^{1/2} - \chi_{AB}^{1/2})^2$; $\chi_{AC} > \chi_{AB}$	1h
	3. $\chi_{AC} > (\chi_{AB}^{1/2} + \chi_{BC}^{1/2})^2$	
B1	$\chi_{AC} < 0$, $\chi_{AB} > 0$, $\chi_{BC} > 0$	2a
B2	$\chi_{AC} > 0$, $\chi_{AB} < 0$, $\chi_{BC} > 0$	2b
B3	$\chi_{AC} > 0$, $\chi_{AB} > 0$, $\chi_{BC} < 0$	2c
C1	$\chi_{AC} > 0$, $\chi_{AB} < 0$, $\chi_{BC} < 0$	3a
C2	$\chi_{AC} < 0$, $\chi_{AB} < 0$, $\chi_{BC} > 0$	3b
C3	$\chi_{AC} < 0$, $\chi_{AB} > 0$, $\chi_{BC} < 0$	3c
D1	1. $\chi_{AB} \leq -(\lvert\chi_{BC}\rvert^{1/2} + \lvert\chi_{AC}\rvert^{1/2})^2$	
	2. $-(\lvert\chi_{AB}\rvert^{1/2} - \lvert\chi_{AC}\rvert^{1/2})^2 \leq \chi_{BC}$; $\chi_{AC} > \chi_{AB}$	4a
	3. $-(\lvert\chi_{AB}\rvert^{1/2} - \lvert\chi_{BC}\rvert^{1/2})^2 \leq \chi_{AC}$; $\chi_{BC} > \chi_{AB}$	
D2	1. $-(\lvert\chi_{BC}\rvert^{1/2} + \lvert\chi_{AC}\rvert^{1/2})^2 < \chi_{AB} < -(\lvert\chi_{BC}\rvert^{1/2} - \lvert\chi_{AC}\rvert^{1/2})^2$	
	1′. $-(\lvert\chi_{BC}\rvert^{1/2} - \lvert\chi_{AC}\rvert^{1/2})^2 \leq \chi_{AB}$; $\chi_{BC} > \chi_{AC}$	
	2. $-(\lvert\chi_{AB}\rvert^{1/2} + \lvert\chi_{AC}\rvert^{1/2})^2 < \chi_{BC} < -(\lvert\chi_{AB}\rvert^{1/2} - \lvert\chi_{AC}\rvert^{1/2})^2$	
	2′. $-(\lvert\chi_{AB}\rvert^{1/2} - \lvert\chi_{AC}\rvert^{1/2})^2 \leq \chi_{BC}$; $\chi_{AB} > \chi_{AC}$	
	3. $\chi_{AC} < -(\lvert\chi_{AB}\rvert^{1/2} - \lvert\chi_{BC}\rvert^{1/2})^2$	4b
D3	1. $-(\lvert\chi_{BC}\rvert^{1/2} - \lvert\chi_{AC}\rvert^{1/2})^2 \leq \chi_{AB}$; $\chi_{AC} > \chi_{BC}$	
	2. $\chi_{BC} \leq -(\lvert\chi_{AB}\rvert^{1/2} + \lvert\chi_{AC}\rvert^{1/2})^2$	4c
	3. $-(\lvert\chi_{AB}\rvert^{1/2} - \lvert\chi_{BC}\rvert^{1/2})^2 \leq \chi_{AC}$; $\chi_{AB} > \chi_{BC}$	

in the infinite molecular weight limit because the enthalpy of mixing but not the combinatorial entropy was taken into account as a condition for compatibility of the blends. Therefore, the miscibility domain obtained was contained by the straight dashed lines shown in Figure 7. We note that if molecular weights are also taken into account, the boundaries are in fact hyperbolic as shown by solid lines in Figure 7. The curves that appear to improve the calculated and experimental agreement were calculated with the values of the χ_{ij} derived by Paul and Barlow as the following ratios: $\chi_{MA\cdot AN}/\chi_{MA\cdot S} = -0.07$, $\chi_{AN\cdot S}/\chi_{MA\cdot S} = 1$. The value of $\chi_{crit}/\chi_{MA\cdot S} = 0.01$ is a best fit value derived in this study from the experimental data. Finally we note that the negative value of $\chi_{MA\cdot AN}$ indicates an attractive interaction between the acrylonitrile and maleic anhydride monomer units.

Conclusion

In this study we have shown miscibility maps whose nature depends on the relationships among the segmental interaction parameters for blends of the two random copolymers $(A_xB_{1-x})_{r_1}$ and $(C_yB_{1-y})_{r_2}$ containing a common monomer unit. The relationships among the intramolecular and intermolecular segmental repulsions (or attractions) are paramount in determining the nature of the miscibility map. When the (absolute) value of the segmental χ_{ij} between different monomer units in at least one of the copolymers is large, the boundaries between the miscibility and immiscibility regions in our representation are given by two straight lines (in the infinite molecular weight limit) or by a hyperbola in the finite molecular weight case. In systems that are immiscible in the infinite molecular weight limit (all χ_{ij} are positive), we find for polymers of finite molecular weight a miscibility region bounded by the x or y axes and one of the following curves: an ellipse, a straight line, or a hyperbola.

Table III summarizes the values of the segmental χ_{ij} obtained from an analysis of the poly(VC-*co*-VAc)/CPVC and poly(VC-*co*-VAc)/poly(Et-*co*-VAc) systems. These values are subject to additional uncertainty because the experiments were of necessity conducted with polymers whose molecular weights and microstructures were nonuniform. In addition, the theoretical model described in the first section contains some oversimplifications as discussed in detail by ten Brinke et al.[20] In particular, the segmental interaction parameters are assumed to be independent of the copolymer composition as well as the polymer concentration. In fact, for homopolymer–homopolymer systems, it has been established that the χ_{ij} are concentration-dependent.[25-28] Nevertheless the overall agreement between the experimental determinations of miscibility domains and those theoretically predicted is excellent. Furthermore in the three χ_{ij}'s relating to VAc interactions (Table III) the progression appears to be consistent with the concept that the ester (or carbonyl) oxygen of VAc interacts attractively with the α-hydrogen

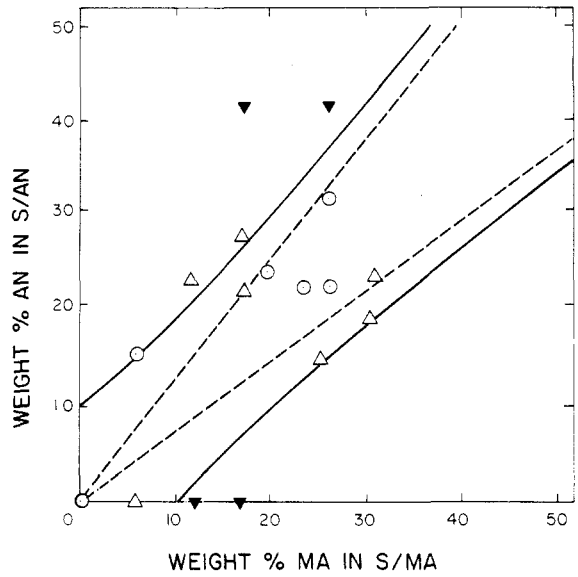

Figure 7. Miscibility map for the blends of poly(S-*co*-MA) and poly(S-*co*-AN). The experimental points were obtained by Hall et al.:[17] (○) miscible; (△) intermediate; (▼) immiscible. The broken lines were calculated with $\chi_{MA\cdot AN}/\chi_{MA\cdot S} = -0.07$ and $\chi_{AN\cdot S}/\chi_{MA\cdot S} = 1$ in the infinite molecular limit by Paul and Barlow.[19] The solid lines were calculated with $\chi_{crit}/\chi_{MA\cdot S} = 0.01$ together with the above ratios.

Table V

Figure	χ_{AB}	χ_{AC}	χ_{BC}
1a	0.200	0.010	0.060
1b	0.119	0.010	0.060
1c	0.100	0.010	0.060
1d	0.020	0.010	0.058
1e	0.010	0.010	0.060
1f	0.040	0.060	0.010
1g	0.021	0.060	0.010
1h	0.005	0.060	0.010
2a	0.060	−0.050	0.070
2b	−0.060	0.050	0.070
2c	0.060	0.050	−0.070
3a	−0.60	0.050	−0.070
3b	−0.060	−0.050	0.070
3c	0.060	−0.050	−0.070
4a	−0.200	−0.010	−0.060
4b	−0.060	−0.010	−0.200
4c	−0.100	−0.010	−0.060

of VC.[29] Finally, it is noted that the accumulation of data represented by segmental χ_{ij}'s is valuable for the prediction of miscible compositions of two copolymers. Such studies can be extended to the general case of copolymer blends not containing a common monomer unit by using the generalized quadratic equation for χ_{blend} derived by ten Brinke et al.[20]

Acknowledgment. This work was supported by DARPA under Contract F49620-85-C-027 and by AFOSR Grant 84-0101. We thank BFGoodrich for supplying the CPVC samples and characterization information and Kuraray and Bayer for gifts of copolymers.

Appendix I

The requirements of the interrelationships of the segmental χ_{ij} for each miscibility map are summarized in Table IV. The conditions 1, 2, and 3 in the table are identical with one another.

Appendix II

The numerical values of the χ_{ij} used in constructing the miscibility maps shown in Figures 1–4 are listed in Table V. χ_{crit} is 0.002 throughout.

Registry No. (Vinyl acetate)·(vinyl chloride) (copolymer), 9003-22-9; (ethylene)·(vinyl acetate) (copolymer), 24937-78-8; (styrene)·(acrylonitrile) (copolymer), 9003-54-7; (styrene)·(maleic anhydride) (copolymer), 9011-13-6.

References and Notes

(1) Paul, D. R.; Newman, S. *Polymer Blends*; Academic: New York, 1978.
(2) Olabisi, O.; Robeson, L. E.; Shaw, M. T. *Polymer–Polymer Miscibility*; Academic: New York, 1979.
(3) Šolc, K. *Polymer Compatibility and Incompatibility*; MMI Press, Hardwood Academic: New York, 1982.
(4) Flory, P. J. *J. Am. Chem. Soc.* **1965**, *87*, 1833.
(5) McMaster, L. P. *Macromolecules* **1973**, *6*, 760.
(6) Patterson, D.; Robard, A. *Macromolecules* **1978**, *11*, 690.
(7) Sanchez, I. C.; Lacombe, R. H. *J. Phys. Chem.* **1976**, *80*, 2352.
(8) Chion, J. S.; Paul, D. R.; Barlow, J. W. *Polymer* **1982**, *23*, 1543.
(9) Stein, D. J.; Jung, R. H.; Illers, K. H.; Hendus, H. *Angew. Makromol. Chem.* **1974**, *36*, 89.
(10) Hammer, C. F. *Macromolecules* **1971**, *4*, 69.
(11) Zakrzewski, G. A. *Polymer* **1973**, *14*, 347.
(12) Goh, S. H.; Paul, D. R.; Barlow, J. W. *Polym. Eng. Sci.* **1982**, *22*, 34.
(13) Alexandrovich, P. R.; Karasz, F. E.; MacKnight, W. J. *Polymer* **1977**, *18*, 1022.
(14) Vukovič, R.; Karasz, F. E.; MacKnight, W. J. *Polymer* **1983**, *24*, 529.
(15) Vukovič, R.; Kuresevič, V.; Segudovič, N.; Karasz, F. E.; MacKnight, W. J. *J. Appl. Polym. Sci.* **1983**, *28*, 3079.
(16) Fried, J. R.; Karasz, F. E.; MacKnight, W. J. *Macromolecules* **1978** *11*, 150.
(17) Hall, W. J.; Cruse, R. L.; Mendelson, R. A.; Trementozzi, Q. A. *Coat. Plast. Prepr. Pap. Melt. (Am. Chem. Soc., Div. Org. Coat. Plast. Chem.)* **1982**, *47*, 298.
(18) Kambour, R. P.; Bendler, J. T.; Bopp, R. C. *Macromolecules* **1983**, *16*, 753.
(19) Paul, D. R.; Barlow, J. W. *Polymer* **1984**, *25*, 487.
(20) ten Brinke, G.; Karasz, F. E.; MacKnight, W. J. *Macromolecules* **1983**, *16*, 1827.
(21) Scott, R. L. *J. Chem. Phys.* **1949**, *17*, 279.
(22) Ueda, H.; Karasz, F. E., to be submitted.
(23) Elmquist, C.; Svanson, S. E. *Eur. Polym. J.* **1976**, *12*, 559.
(24) Fredriksen, O.; Crowo, J. A. *Makromol. Chem.* **1967**, *100*, 321.
(25) Kwei, T. K.; Nishi, T.; Roberts, R. F. *Macromolecules* **1974**, *7*, 667.
(26) Su, C. S.; Patterson, D. *Macromolecules* **1977**, *10*, 708.
(27) Hadziioannou, G.; Stein, R. S. *Macromolecules* **1984**, *17*, 567.
(28) Shiomi, T.; Kohno, K.; Yoneda, K.; Tomita, T.; Miya, M.; Imai, K. *Macromolecules* **1985**, *18*, 414.
(29) Coleman, M. M.; Zarian, J. *J. Polym. Sci., Polym. Phys. Ed.* **1979**, *17*, 837.